SPECIAL ASPECTS OF THE CENTRAL PART
OF FILCHNER-RONNE ICE SHELF, ANTARCTICA

by

F. Thyssen

(Forschungsstelle für physikalische Glaziologie der Westfälischen Wilhelms-Universität,
Corrensstraße 24, D – 4400 Münster, Federal Republic of Germany)

ABSTRACT

Aero-measurements during the 1983–84 and 1985–86 field seasons showed that the ice in the central part of Filchner—Ronne Ice Shelf is more than 250 m thicker than has been assumed previously. In the margin area a double layering of the ice was found, with disappearing bottom reflections farther inland. High absorption of approximately 0.3 dB/m in the lower layer and a decreasing reflectivity at the ice / sea-water interface, probably caused by bottom freezing, have been estimated. Aero-measurements were used to map the surface elevation of the ice, with an accuracy of approximately 3 m. From the plot of ice thickness against surface elevation it was possible to obtain a calibration curve for isostatic conditions. Large deviations from this plot with an ice thickness which is apparently too small (they seem to be isostatic anomalies) were found in the central part of the ice shelf. The true ice thickness could easily be calculated and mapped from these anomalies and the electromagnetically measured thickness.

From the map based on flights made in 1983–84 the site for a bore hole was chosen in the central part of the ice shelf with an estimated ice thickness of about 450 m, instead of the less than 200 m deduced by an electromagnetic reflection (EMR) method. Hot-water drilling by the ground party of our group (H. Engelhardt and J. Determann) revealed an ice thickness of 465 m at this site.

INTRODUCTION

In 1983 Robin and others published an up-to-date compilation of geophysical results for Filchner—Ronne Ice Shelf. What was most difficult to understand, and what therefore provided the motivation for the following programme, was the glaciological situation in the central part of this ice shelf. Remarkably small ice thicknesses in the central ice shelf (sometimes less than 200 m) were found by electromagnetic reflection (EMR) profiling. This area was bounded laterally by ice more than 500 m thick, giving a strong gradient in ice thickness nearly perpendicular to the assumed flow lines of the adjacent ice streams. Robin could not offer a definitive explanation for this observation but hypothesized the presence of a layer of saline ice.

The data field used in the paper by Robin and others (1983) was adequate.

In 1983–84 the aircraft *Polar 2* was equipped with our electromagnetic reflection system, precision radar and barometric altimeters, and a doppler navigation system supported by Omega data. It flew at a nearly constant pressure level over Filchner—Ronne Ice Shelf, mainly along north—south profiles. Whenever possible, the levelling system was calibrated over the sea at the beginning and end of flights.

The electromagnetic aero-measurements were made mostly at 35 MHz mean frequency, with a 7 kW peak pulse and different pulse lengths between 100 and 500 ns. EMR signals at a rate of 4/s and the actual navigation data set at a rate of 1/s were digitally recorded.

OBSERVATIONS

The results from the 1983–84 field season showed for the first time that the ice in the central part of Filchner—Ronne Ice Shelf is more than 250 m thicker than has been assumed previously.

A first map of ice thickness, together with other parameters of the basal layer, was presented at the Filchner workshop held in Bremerhaven in 1985 (Thyssen 1985). It has been published in the third Filchner—Ronne Ice Shelf Programme report (Thyssen 1986).

A detailed programme for the 1985–86 field season was developed and carried out in order to verify these results. The programme included an extension of the aero-measurements, reflection seismics on a mainly north—south profile (using a newly developed streamer), high-resolution EMR ground measurements which continued the field work of 1983–84, and an access bore hole.

From the ice-thickness map based on flights made in 1983–84, the site for the access bore hole was chosen in the central part, with an estimated ice thickness of approximately 450 ± 50 m, instead of less than 200 m as deduced from EMR. Hot-water drilling, by the ground party of our group (H. Engelhardt and J. Determann) in 1986, revealed an ice thickness of 465 m at this site, with indications of a mixture of ice and sea-water at the ice / sea-water interface (Engelhardt and Determann 1987). The results from the 1983–84 flights were supported by seismic reflections from the same area (Determann and others 1988, this volume).

The data field of the 1985–86 aero-measurements increases the accuracy of electromagnetic ice-thickness and elevation measurement because the spacing of the flight tracks was narrower and there was more advanced calibration of the levelling system over sea and over clean ice in mirror conditions.

Surface elevation and reflection travel times can be evaluated from the recorded data set. A velocity—depth function derived by N. Blindow from electromagnetic common mid-point profiles at Filchner Station (Blindow, unpublished) was used over the whole ice shelf to transform the measured travel times into depths.

The ice thickness in areas where the ice—water interface was clearly reflected could be measured with an accuracy of approximately 5 m without further processing. Aero-measurements were used to map the surface elevation of the ice with an accuracy of approximately 3 m.

The evaluation of the aerogeophysical measurements provided some new and remarkable results:

Up to a distance of 10–20 km from the ice front the ice shelf consists of clean ice, with a strong reflectivity close to unity at the bottom (mirror condition).

Farther inland, at distances of 30–50 km in the central part of the area under investigation, double layering of the ice was found, with disappearing bottom reflections, on all records. Figure 1 shows an example of the 1983–84 results. The record was corrected for changes in flight level. The small down-doming in the crevasse area was ignored in the processing.
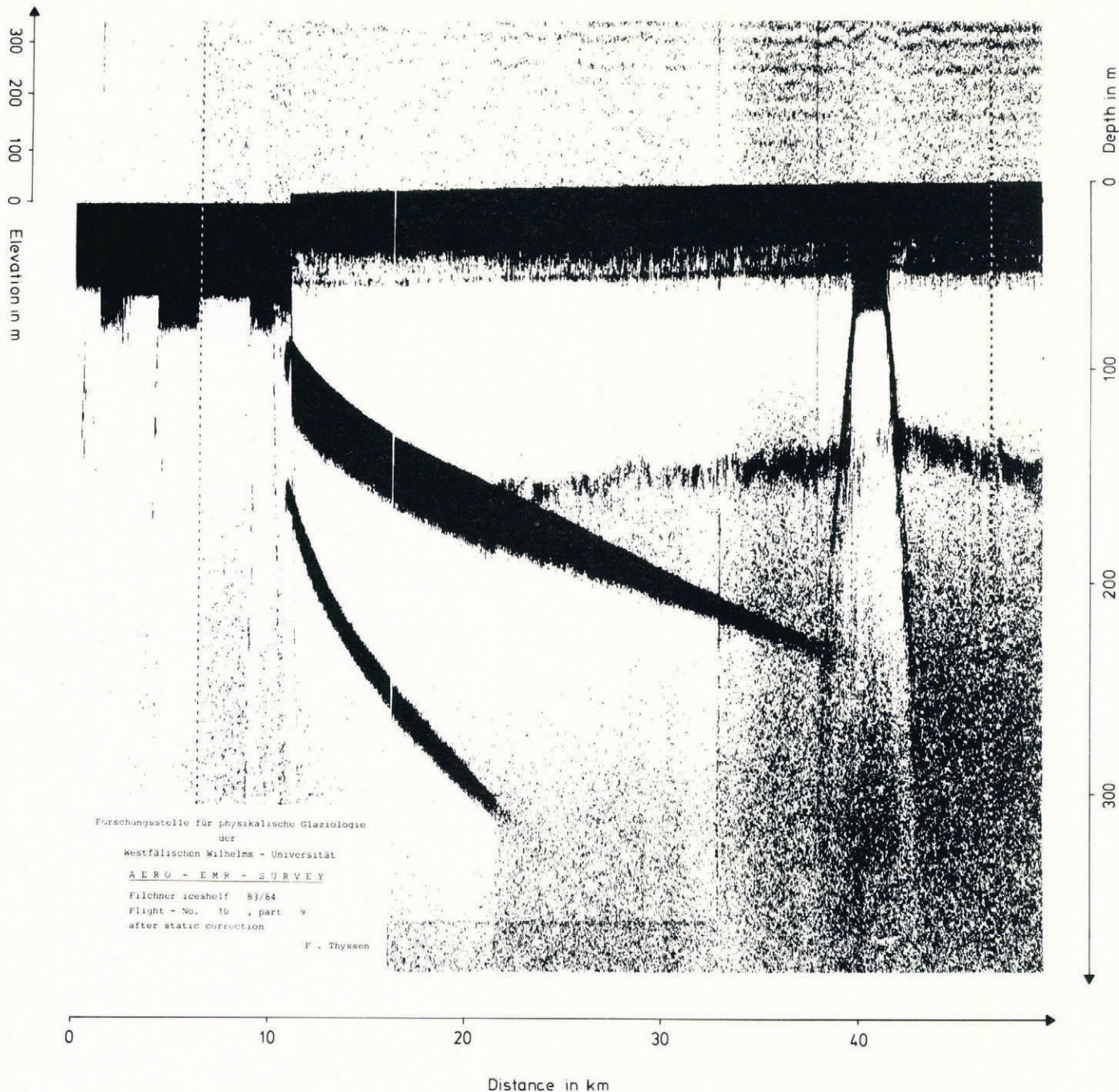
Fig. 1. Example of double layering with a disappearing reflector farther inland; the record of 1983–84 has been corrected for changes in flight level.

From the slope of the bottom reflection in all records from this area it is inferred that bottom melting is not substantially higher in the basal layer than in the upper clean-ice layer.

In some of the records which show a double layering, the bottom reflector fades farther inland, although the total thickness of the basal layer remains nearly constant. This indicates that the power returned from the ice–water interface diminishes strongly. A weak reflecting and strongly absorbing ice / sea-water mixture, caused by freezing, can be assumed at this boundary, and/or there is an increase in the salinity of ice in the up-stream direction.

The internal reflector has a complicated structure. In some areas it is smooth and well developed. In other areas it shows numerous diffraction hyperbolas which are separated from each other (Fig. 2).

From the changes in amplitude of the reflected signals at different thicknesses of the basal layer, the absorption can be estimated by making the following assumptions: (a) a mirror-like reflector normally found in clean ice in melting conditions with a constant reflection coefficient near unity at the bottom; (b) no scattering in the basal layer; (c) negligible differences in reflection losses between clean and basal ice (this is a usual situation).

On the basis of these assumptions the absorption is estimated to be approximately 0.3 dB/m at 35 MHz. This value can be attributed to a d.c. resistivity of the order of 2 kohm m.

A calibration curve for isostatic conditions can be obtained from the plot of the surface elevation of the floating ice (freeboard) against ice thickness, measured in areas of clean ice with mirror conditions at the ice / sea-water interface.

All data points evaluated from reflections of the bottom of the basal layer are situated slightly but systematically below this curve, indicating a slightly higher density for this ice and higher electromagnetic absorption. The thickness of this lower layer was derived by assuming
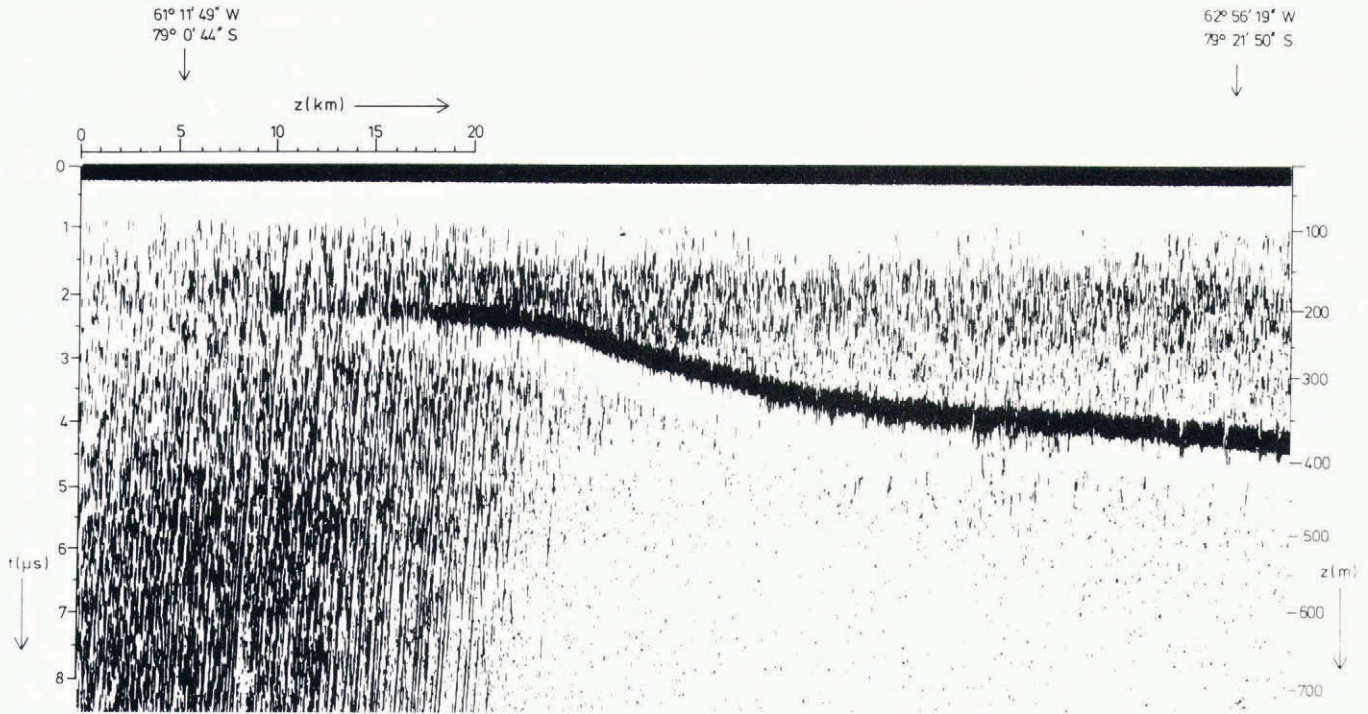
61° 11′ 49″ W
79° 0′ 44″ S

62° 56′ 19″ W
79° 21′ 50″ S

Fig. 2. Example of a profile, showing the internal layer with a steep increase north of Henry Ice Rise (indicated as A–B in the map of flight tracks, Fig. 4).

an electromagnetic wave velocity for clean ice which can be expected to be too large (up to now, there have been no measurements of velocities in the basal layer). It can be estimated that the basal ice is denser by about 5% than normal ice in these conditions.

Large positive deviations from this plot (with an ice thickness which is apparently too small) can be found in the central part of the ice shelf. These anomalies may be caused either by ice rumples (normally indicated by a slightly higher surface elevation) or by the ice thickness which was derived electromagnetically being too small. The thickness of the saline ice can be calculated from the latter apparently isostatic anomalies, assuming the same density for saline and clean ice.

The plot of ice thickness H in areas without a basal layer and with clean conditions, against surface elevation (freeboard) without correction of barometric changes h, is shown in Figure 3.

The linear part of this plot for ice thicknesses of over 100 m can be expressed by the following formula:

$$h = (0.1130 \pm 0.0012)H + (13.40 \pm 0.3) \qquad (1)$$

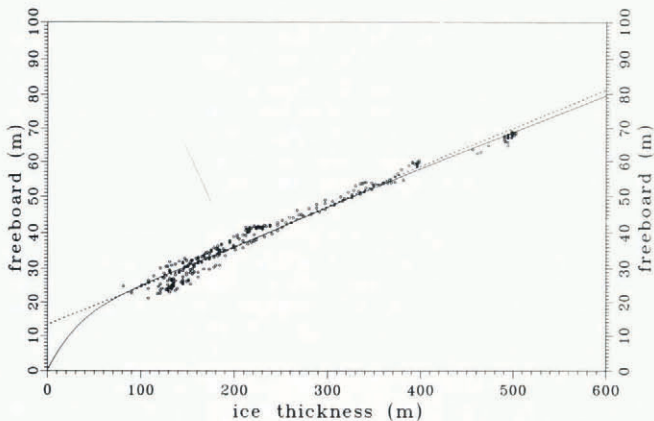where h and H are expressed in metres.

An equivalent relation can be calculated by using the depth–density curves from Herron and Langway (1980), with an accumulation rate of $0.17\,m_{H_2O}/a$, a mean annual temperature of $-26.5\,^{\circ}C$ (Reinwarth and Graf 1985) and an initial density of $0.46\,Mg\,m^{-3}$. This curve is plotted as an unbroken line in Figure 5.

Following Coslett and others (1975), Equation (1) can be expressed in terms of the density of pure ice ρ_i and of
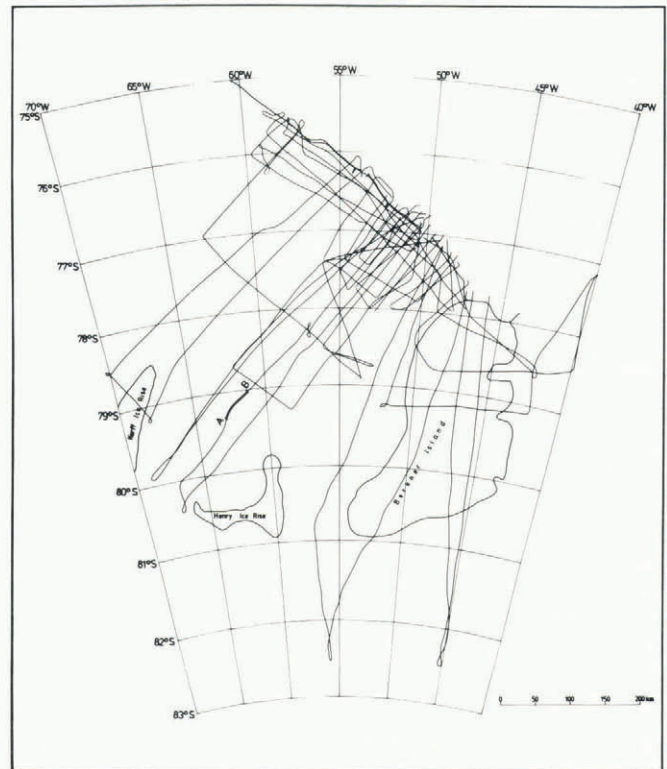

Fig. 3. Isostatic plot for clean ice in mirror conditions.

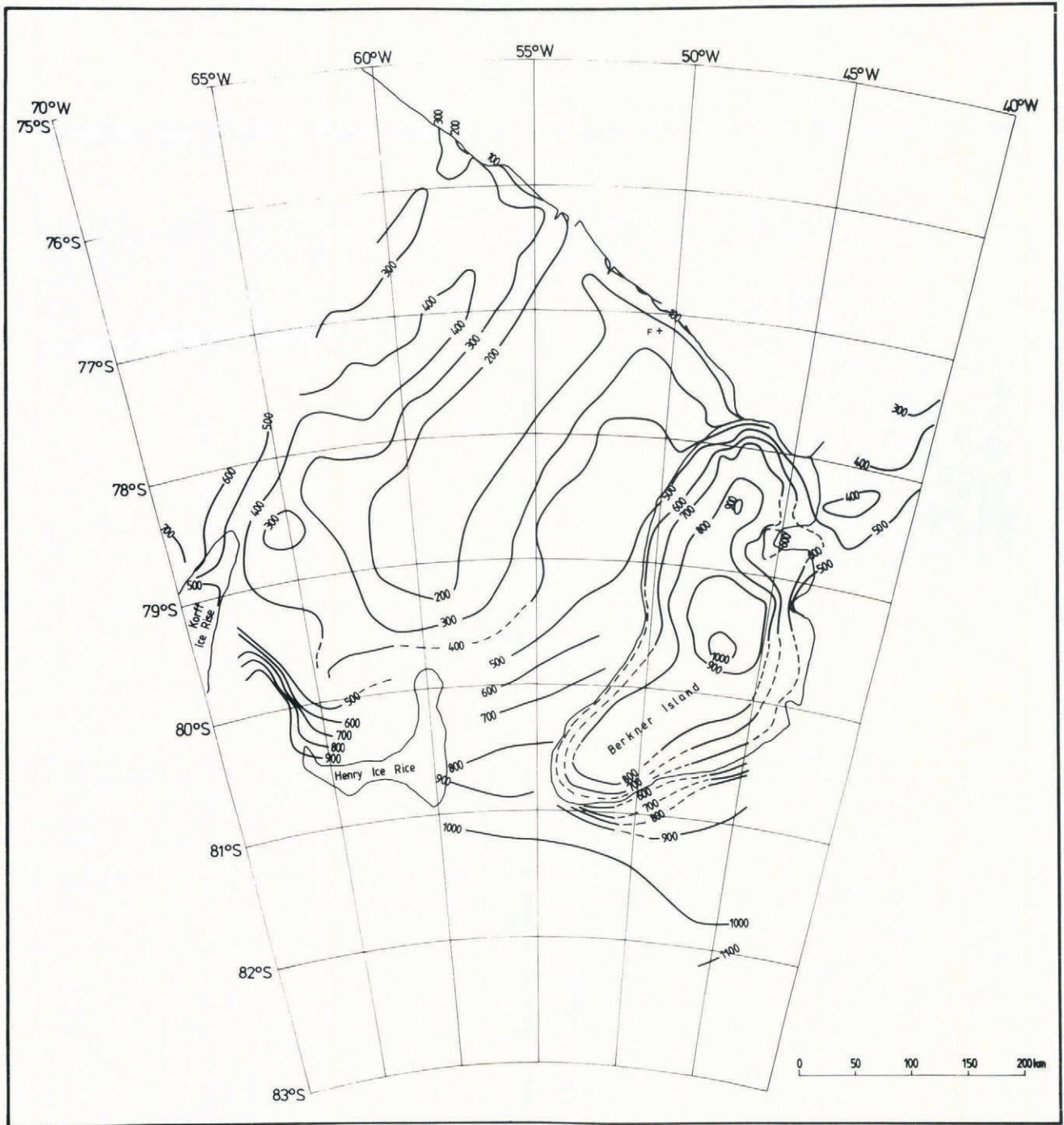Fig. 4. Map of flight tracks for the 1983–84 and 1985–86 field seasons.

Fig. 5. Map of EMR ice thickness or internal reflectors in the central part of Filchner—Ronne Ice Shelf.

sea-water ρ_w, and the air content can be measured as an equivalent length of air C (m):

$$h = (1 - \rho_i/\rho_w)H + C\rho_i/\rho_w \qquad (2)$$

Where the density of pure ice is 0.917 Mg m^{-3}, this results in a value of 1.0338 ± 0.0014 Mg m^{-3} for the mean density of the ocean water in that area, which is remarkably high. A value of 15.11 ± 0.34 m can be derived for C.

From this isostatic plot it is possible to reduce pressure changes during flight time, comparing elevation (as the difference between barometric altitude at a nearly constant pressure level) and radar-altimeter data with the elevation deduced from the thickness of clean ice in mirror conditions. The elevation of areas of saline ice surrounded by clean ice can easily be interpolated.

MAPPING OF THE RESULTS

A map of our flight tracks for the field seasons 1983—84 and 1985—86 is given in Figure 4. The map for the lowest reflector (either internal or from the real bottom), derived from the electromagnetic data from both field seasons, differs from the maps of Robin (1983) and Crabtree and Doake (1986) only in detail, mainly the result of different flight tracks and spacing. This is shown in Figure 5.

A map of the elevations of the central part of Filchner—Ronne Ice Shelf was produced from the combined results of the 1983—84 and 1985—86 field seasons with an accuracy of ±3 m, and is presented in Figure 6. The accuracy of the elevation is estimated from 57 crossings of profiles at 3 m.

In this surface-elevation map a small up-doming of approximately 5 m can be seen north of the eastern part of Henry Ice Rise. It is not clear at this time whether this is an ice rumple or a very strong local accumulation of saline
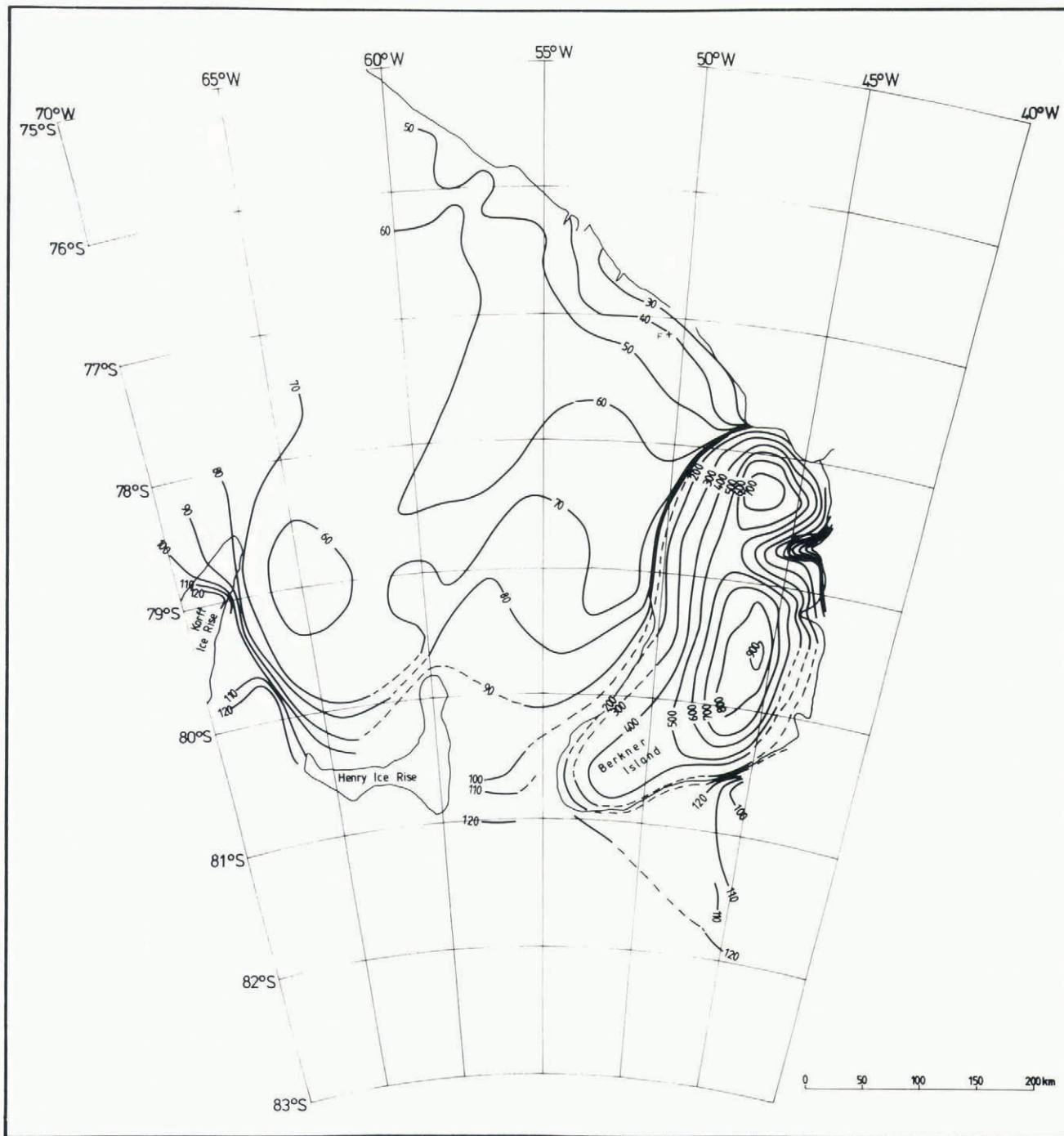
Fig. 6. Map of surface elevations of the central part of Filchner–Ronne Ice Shelf.

ice. Figure 2 shows a profile measured in this area, running from south to north (indicated as A–B on Fig. 4) with a very steep increase (of 150 m over 15 km) in the depth of the internal layer. A large area of broken ice lies immediately to the north and north-west of this area.

A map of the apparent and real isostatic anomalies (Fig. 7) is derived from the differences between measured elevation and elevation calculated from the EMR ice thickness (Fig. 5) using Equation (1). There is still an uncertainty in the area north of Henry Ice Rise, as mentioned above. One possible explanation of the apparent isostatic anomalies is that ocean currents beneath the ice shelf are accumulating saline ice at a rate which in certain areas is much higher than the accumulation on the surface.

The large apparent anomalies of elevation in the central part of the ice shelf indicate thick ice. The real ice thickness can easily be derived from the surface elevation by reference to Figure 6. The result is shown in Figure 8. The data field was enlarged by using measurements from a more westerly part of the ice shelf where Crabtree and

Doake (1986) carried out electromagnetic measurements on a thin-ice area. In this area an isostatic anomaly can be found in the map in Figure 7, indicating much thicker ice than was measured by EMR soundings in this area.

The ice thickness lies well within the error range of the first map (published in 1986), and agrees with the results of the access bore hole and the seismic-reflection work which was carried out in 1985–86 in the same area. The accuracy is affected by the irregular distribution of flight tracks and by errors in surface elevation and in reflection time. It can be estimated at ±30 m for ice with a basal layer and at ±5 m for clean ice.
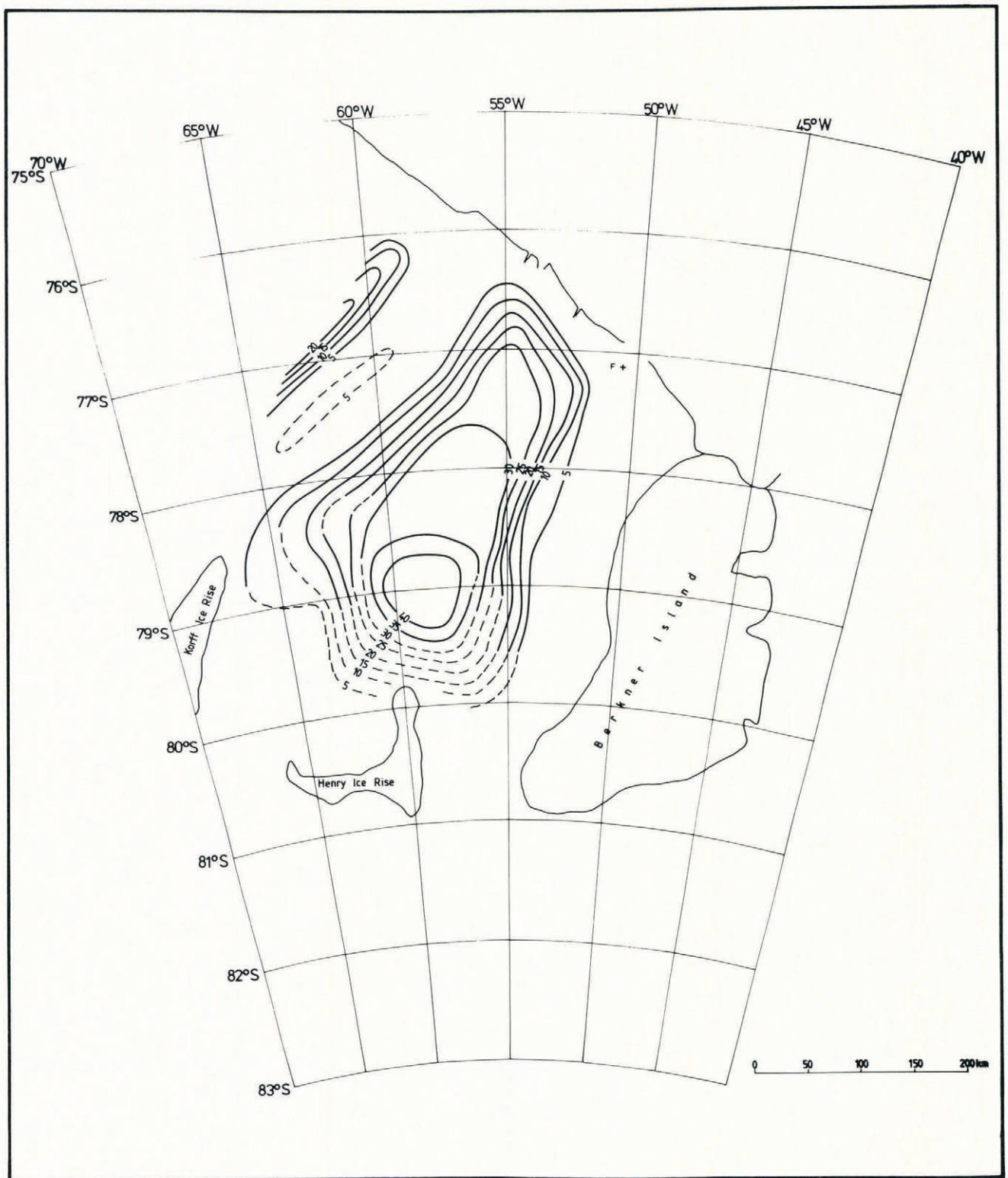
Fig. 7. Map of apparent and real isostatic anomalies (in metres altitude).

REFERENCES

Blindow, N. Unpublished. Bestimmung der Mächtigkeit und des inneren Aufbaus von Schelfeisen und temperierten Gletschern mit dem hochauflösenden elektromagnetischen Reflexionsverfahren. (Dissertation, Westfälische Wilhelms-Universität, Münster, 1986.)

Coslett, P.H., M. Guyatt, and R.H. Thomas. 1975. Optical levelling across an Antarctic ice shelf. *Br. Antarct. Surv. Bull.*, 40, 55-63.

Crabtree, R.D., and C.S.M. Doake. 1986. Radio-echo investigations of Ronne Ice Shelf. *Ann. Glaciol.*, 8, 37-41.

Determann, J., F. Thyssen, and H. Engelhardt. 1988. Ice thickness and sea depth derived from reflection-seismic measurements on the central part of Filchner–Ronne Ice Shelf, Antarctica. *Ann. Glaciol.*, 11, 14-18.

Engelhardt, H., and J. Determann. 1987. Borehole evidence for a thick layer of basal ice in the central Ronne Ice Shelf. *Nature*, 327(6120), 318-319.

Herron, M.M., and C.C. Langway, *jr.* 1980. Firn densification: an empirical model. *J. Glaciol.*, 25(93), 373-385.

Reinwarth, O., and W. Graf. 1985. Neuere Untersuchungen zur Akkumulation auf dem Filchner/Ronne-Schelfeis. *In* Kohnen, H., *comp. Filchner-Ronne-Ice-Shelf-Programme. Report No. 2.* Bremerhaven, Alfred-
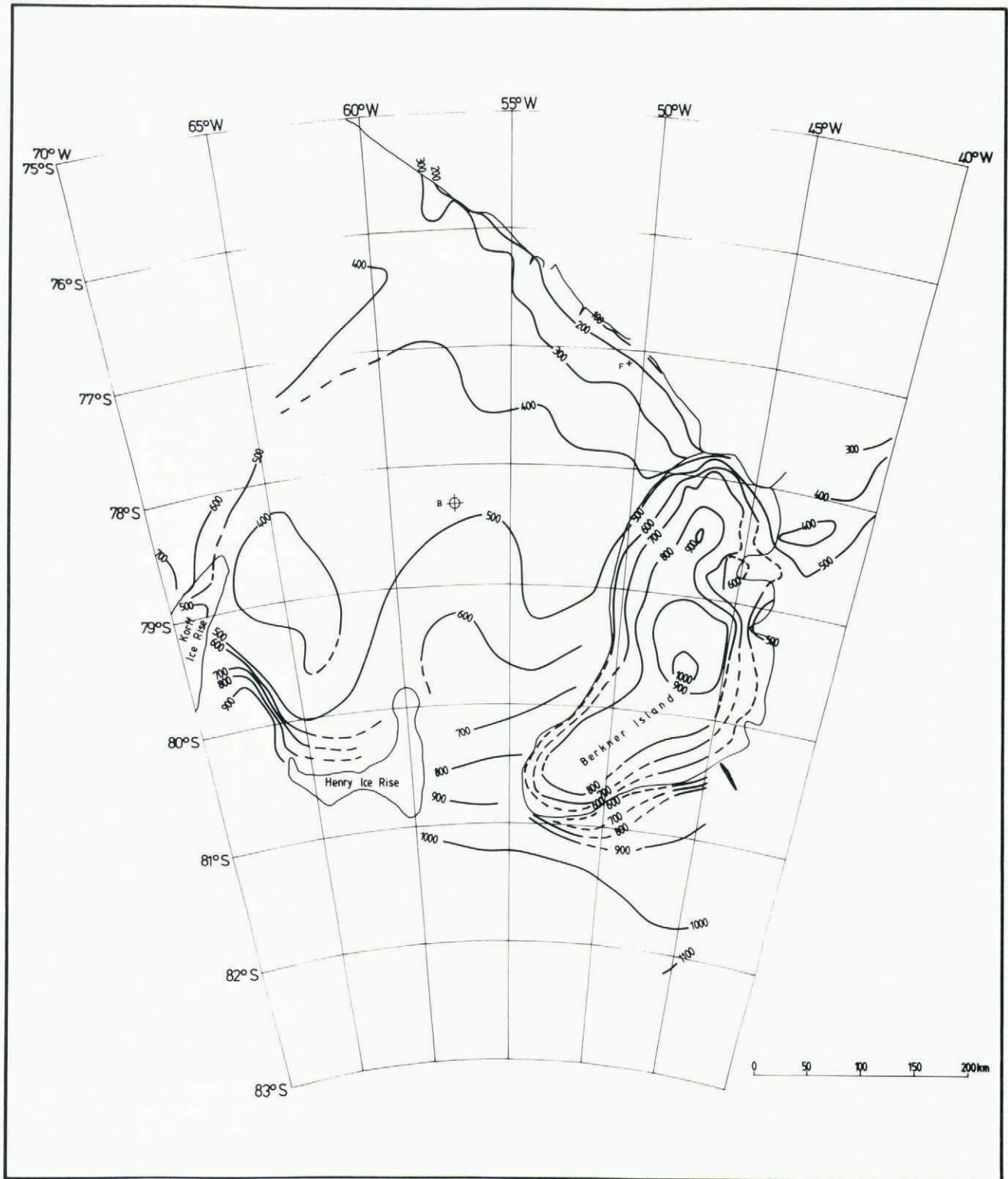
Fig. 8. Ice thickness of the central part of Filchner−Ronne Ice Shelf, compiled from the map of apparent isostatic anomalies and from reflections.

Wegener-Institute for Polar Research, 7-17.

Robin, G. de Q., C.S.M. Doake, H. Kohnen, R.D. Crabtree, S.R. Jordan, and D. Möller. 1983. Regime of the Filchner−Ronne ice shelves, Antarctica. *Nature*, 302(5909), 582-586.

Thyssen, F. 1985. First results from Polar-2-measurements on the Filchner and Ekström ice shelves. *In* Kohnen, H., *comp. Filchner-Ronne-Ice-Shelf-Programme. Report No. 2.* Bremerhaven, Alfred-Wegener-Institute for Polar Research, 131-132.

Thyssen, F. 1986. The central part of the Filchner/Ronne Ice Shelf. *In* Kohnen, H., *comp. Filchner-Ronne-Ice-Shelf-Programme. Report No. 3.* Bremerhaven, Alfred-Wegener-Institute for Polar and Marine Research, 81-83.